KSABC
The Korean Society for Applied Biological Chemistry

ARTICLE   **Open Access**

Detoxifying and antioxidant effect of ellagic acid nano particles in rats intoxicated with sodium nitrites

Amira Ragab EL Barky[2], Tarek Mostafa Mohamed[2] and Ehab Mostafa Mohamed Ali[1,2]*

Abstract

Sodium nitrite is used as a preservative in food products to stabilize color and reduce rancidity. Its absorption into the body causes many diseases. Ellagic acid is a natural polyphenol that contains powerful antioxidants, but it is taken as a poorly absorbed food. Therefore, chitosan-coated nanoparticles (EANP@CS) were loaded to enhance their bioactivity and bioavailability after oral administration. EANP@CS was administrated in rats given water containing sodium nitrite to reduce toxins. Ellagic acid was extracted from pomegranate and manufactured EANP@CS. EANP@CS was identified by FT-IR, UV, X-ray diffraction and TEM. Average EANP@CS size ranges from 20–62 nm. Rats were divided into five groups: normal, treated using EANP@CS; rats were receiving nitrite for 8 weeks, and the last two groups were treated with EANP@CS. Serum and liver NO, MDA, and DNA fragmentation were reduced. Liver thiol and GSH levels, and Gpx, catalase and GST activities increased in rats treated with EANP@CS rats compared to rats drinking nitrites. Liver NOS activity was reduced 7 and 4.9 times in rats treated with EANP@CS during or after discontinuation of nitrite administration, respectively. Liver arginase activity was raised in rats that drink nitrite or were treated using EANP@CS. Inflammatory infiltrations of the liver, kidney, and spleen were observed in the tissues of rats that received nitrites and improved when the rats were given EANP@CS. EANP@CS improved oral bioavailability and reduce the risk of sodium nitrite in rats. EANP@CS can be used as a therapeutic goal to detoxify any unwanted toxic substance in food.

Keywords: Sodium nitrite, Ellagic acid, Nanoparticles, Chitosan, Nitric oxide, Antioxidant

Introduction

Sodium nitrite is used to stabilize meat color and reduce rancidity by inhibiting lipid peroxidation and growth of microorganisms on food. Nitrites are used in the medical field such as vasodilator, bronchodilator, and detoxifying of cyanide poisoning. But the use of nitrite leads to human exposure to many diseases [1].

Sodium nitrite is one of the causes of colorectal cancer. Sodium nitrite is added to preserved meat or any other foods to prevent the growth of microorganisms such as *Clostridium botulinum* [2]. Sodium nitrite consumption can lead to the formation of N-nitroso compounds that are carcinogenic [3]. The oral route is the main way of taking sodium nitrite; it affects the gastrointestinal tract and small intestine. The acidic medium of the gut leads to the conversion of nitrite to a nitrosating agent that may end up forming nitrosamine. Also, peroxenitrate and nitryle chloride may be produced which is more harmful than nitrite itself and can act as direct mutagens [4].

Pomegranate (Punica granatum L.) is an edible fruit, which is an anti-oxidant and contains polyphenols, ascorbic acid, vitamins, and minerals [5]. Ellagic acid (EA) found in pomegranate, with about 13% of peel extracts [6]. Ellagic Acid is a powerful anti-oxidant, antibacterial, antiviral and anti-inflammatory compound. It also has anti-proliferative and upregulated tumor suppressor genes and apoptotic genes in

*Correspondence: emali@kau.edu.sa; ehab_1964@hotmail.com; ehab.ali@science.tanta.edu.eg
[1] Biochemistry Department, Faculty of Science, King Abdulaziz University, Jeddah, Saudi Arabia
Full list of author information is available at the end of the article

EL Barky *et al. Appl Biol Chem*   (2020) 63:47

Page 2 of 16

cancer cells [7]. Ellagic acid is taken with many drugs that cause oxidative stress [7, 8]. Ellagic acid is insoluble in water, so it has low bioavailability, because of its metabolites, and is quickly eliminated. So its therapeutic advantage is restricted because most clinical drugs are administered orally [9].

Chitosan is a polymer compound derived from chitin by N-deacetylation. It is commonly used in food, bioengineering, enzyme loading, drug conduction carrier, plant growth factor, and antimicrobial. It has the property of biodegradation, and biological compatibility and activity, [10]. Chitosan nanoparticles are more precisely applied to cells, and positively charged chitosan nanoparticles give greater convergence to negative-charge biological membrane and site-specific site targeting, allowing their use as drug-coated materials, to accelerate drug release in a target cells. Chitosan nanoparticles are used in the food industry to control food stability [11].

Ellagic acid nanoparticles that are coated with chitosan polymer lead to increased absorption and delivery of the ellagic acid (EA) to the target cells. Chitosan-coated ellagic nanoparticles (EANP@CS) can increase EA stability and improve drug absorption, have been used as a system to release the drug and provide an appropriate dose of the drug to the target tissues. EANP@CS increases the affinity of these nanoparticles with protein receptors in the target cells and may prevent the accumulation of EA molecules [12].

This study aimed to extract EA from pomegranate and convert it into nanoparticles with the help of chitosan polymer (EANP@CS) to enhance biological availability. Antioxidants, nitric oxide, NOS, arginase, and DNA fragmented were then evaluated in the liver and kidney to study the efficacy of EANP@CS in rats intoxicated with sodium nitrite.

Materials and methods
Extraction of ellagic acid
Ellagic acid was extracted from the pomegranate peel powder (Punica granatum), the pomegranate peel was purchased from the Egyptian market and was recognized by the Faculty of Science, University of Tanta (Herbarium- TANE, Index Herbariorum New York Botanical Garden), according to Lu and Yuan [13] with some modification. In brief, ground crushed pomegranate peel was immersed in 60% aqueous ethanol and stirred over a hot plate with a stirring The tannin that results from this extract was filter and hydrolyzed by 5% H_2SO_4 for 5 h and left overnight. The dark brown crude precipitate EA was collected and dissolved in ethanol, filtered and left to dry in the oven at 50°C.

Synthesis of EA nanoparticles coated with chitosan (EANP@ CS)
EANP@CS was synthesized using sodium triphosphate as a gelatin agent with some modification. Chitosan polymer (MW = 60–90 kDa, ≥ 85% decyl, sigma) was dissolved in 2% glacial acetic acid. The mixture of chitosan and glacial acetic acid was stirred overnight at ambient temperature and the pH was adjusted to 5.0 using sodium hydroxide 1 M. Ellagic acid was dissolved in 0.5% dimethyl sulfoxide (DMSO), added to the fresh chitosan dispersion and stirred for about an hour. An equal amount of sodium tripolyphosphate (Sigma Aldrich, USA) 1 mg/mL was added drop wise to the CS-EA solution under moderate stirring. The obtained mixture was stirred for 1 h to form EA coated chitosan nanoparticles. EANP@CS was separated by centrifugation. The pellets were collected and stored at −20°C for further use [14].

Identification of ellagic acid and EANP
Fourier transforms Infrared spectroscopy (FT-IR)
To identify the functional groups of the active compound, an infrared spectroscopy (Model-JASCO FT-IR 4100 LE, made in Japan, range: 4000–400 cm -1) was performed in the infrared field in the (Microanalytical Unit, Faculty of Science, Tanta University, Egypt). The extract of Ellagic Acid and EANP @ CS (1–2 mg) was ground to a powder with mortar and mixed with KBr (3–4 mg).

Ultraviolet spectroscopy (UV)
Absorption of ellagic acid and EANP @ CS extract was determined by a double visible UV spectrophotometer in the ultraviolet region (200 nm–800 nm) at a 5 nm interval and readings versus blank. The graph is drawn between absorption and wavelength to determine the maximum wavelength for ellagic acid and EANP@CS (Microanalytical Unit, Faculty of Science, Tanta University, Egypt).

X-ray diffraction
X-ray diffraction patterns for EA and EANP@CS (Philips, Netherlands) were recorded with Cu Kα (1.5418 Å) as the source and the spectrum was collected with an average scanning rate of 10 per min.

Transmission electron microscopy (TEM)
Transmission electron mcroscopy (TEM) was taken to capture different image snapshots of EANP@ CS. EANP@CS image size determined using JEM 2010F electron microscope with 200 kV operating voltage (JEOL, Ltd., Tokyo, Japan). EANP@CS was

EL Barky *et al. Appl Biol Chem* (2020) 63:47

Page 3 of 16

ultrasonicated for 30 min, one drop of ellagic acid nanoparticle sample was placed on the smooth film of carbon-coated TEM copper grid and dried. A drop of 0.5% of phosphotungstic acid was diffused on the TEM grid.

Experimental animals

Fifty adult white male albino Wister rats, 3-4 months old with an average body weight of 180–200 g, were used in the experimental study. The mice were purchased from the Animal House at Tanta University, Egypt. The mice lived in a specially controlled room. The rats were treated according to the instructions of the Animal Ethics Committee (Tanta University, Egypt). The animals were adapted 2 weeks before the experiment.

Rats were divided into two main groups: the normal group and the sodium nitrite group, the normal group was subdivided into control rats that did not receive any drugs (GI), the normal rats received EANP@CS (G. II), the rats were received orally EANP@CS (20 mg/kg b.Wt.) 4 day/week [15]. The sodium nitrite group was divided into three subgroups, the untreated nitrite group (G. III) (rats received 2 g/L nitrite in drinking water for 8 weeks) [16], Sodium nitrite and EANP @ CS treated during drinking (G. IV) (rats received nitrite in drinking water at 2 g/L concentrations for 8 weeks, and treated with EANP@CS orally 4 days/weeks in the last 4 weeks). The Last one sodium nitrite and EANP@ CS treated after stopping sodium nitrite (G. V) (rats treated with EANP@CS orally 4 days/weeks in the last 4weeks; (rats received 2 g/L nitrites in the drinking-water for 4 weeks and then treated with EANP@ CS 4 days/weeks in the last 4 weeks). The nitrite was replaced by drinking water in the last 4 weeks in G.V.

By the end of 8 weeks, the rats fasted overnight, then anesthetized and sacrificed. Blood was collected plasma and serum were separated. The serum was used for evaluated various biochemical parameters. The liver, kidney and spleen were separated and washed with saline. Part of the liver and kidney samples were homogenized at 4° C. The second part was fixed in formalin for 24 h and then stained with hematoxylin and eosin [17].

Determination of Hemoglobin; urea level, ALT and AST activities

Hemoglobin level was measured. Serum urea level as a biomarker for kidney disease, ALT and AST activities for liver disease were determined by using kits purchased from Randox Labs, UK. Liver and kidney protein were measured [18].

Determination of L- MDA; GSH, total protein thiol (PTH) and non-protein thiol (NPTH) levels; Gpx; GST and catalase activities

The concentration of liver and kidney L-MDA was evaluated by the reaction MDA with thiobarbituric acid (TBA) which gives a pink color. The pink color is extracted by n-butanol and measured at 532 nm. The MDA level was calculated using molar absorptivity according to Draper and Hadley [19].

Glutathione levels were measured in the liver and kidneys by the interaction of 5, 5´- dithiobis-2-nitrobenzoic acid (DTNP) with GSH at pH 8.2. The obtained yellow color was read at 412 nm. The level of GSH in the liver or kidney was calculated using the standard curve for different known GSH concentrations ranging from 0.25 to 5 mM [20]. Total protein thiol (PTH) and non-protein thiol (NPTH) were performed in the liver and kidney. Thiol reacts with DTNB (5, 5-Dithiobis (2-nitrobenzoic acid) in the presence of pH Tris-buffer 8.2 and methanol, and absorption was measured at 412 nm [21].

Glutathione peroxidase (Gpx) activity was determined in liver and kidney after the consumption of GSH and H_2O_2 to form GSSG. In summary, a mixture of GSH, H_2O_2, EDTA salt, sodium azide, 10% liver and kidney homogenate, and distilled water were incubated for ten minutes. The GSH decrease was determined by the Ellman method and Gpx activity was expressed as nmole/min/mg [22]. Liver and kidney glutathione S- transferase (GST) activity was determined by kinetic method. In brief, 1-Chloro-2, 4-dinitrobenzene (CDNB, Sigma-Aldrich) was coupled with reduced glutathione (GSH, Sigma-Aldrich) in a quartz cuvette, this coupling leads to a marked increase in measured absorption, and the reaction was done in the presence of 0.05 M buffer potassium phosphate pH 7.4 [23]. Liver catalase was determined by the H_2O_2 degradation rate at 240 nm. The unit of the catalase enzyme was expressed by mmol of the consumed H_2O_2/min/mg protein [24].

Determination of serum, liver and kidney NO, liver NOS, liver and kidney arginase activities and DNA fragmentation

Serum, liver, and NO were determined after converting nitrate to nitrite using cadmium. Total nitrite was determined by Griess's reagents. The level of nitric oxide (NO) (nitrite and nitrate) was determined in the blood serum and liver homogeneity as described previously [25]. Briefly, 30% of zinc sulfate was added to the serum or 10% of the liver homogenate to precipitate the protein. After centrifugation, 100 μL of supernatant was added to 0.5 g granulated cadmium and 0.4 mL of deionized water. After overnight rotating and centrifugation, 0.25 mL of the final supernatant was completed with distilled water,

EL Barky *et al. Appl Biol Chem*   (2020) 63:47

Page 4 of 16

after which Griess's reagent contained 1 g/L sulphanilamide, 25 g/L phosphoric acid and 0.1 g/L N-1-naphthylethylen diamine reacted with nitrites measured at 540 nm. The sum of total nitrites (NO) was studied by the aiding of the nitrites standard curve (5 to 100 μM).

The activity of liver nitric oxide synthase (NOS) was determined by releasing nitric oxide from ʟ-arginine A reaction mixture contained 3.4 mM of arginine, 2 mM of tetrahydrobiopterin, 0.5 mM of FAD, 12 mM of NADPH^{+}, 50 μL of 20 mM CaCl$_2$, 50 μL of 40 mM of dithiothreitol, the reaction was completed to 1 mL with 0.1 M Tris–HCl buffer, pH 7.5 after adding 50 μL of 10% liver homogenates and incubated at 37 ° C for 3 h [26]. Total nitrites were measured in the reaction and subtracted from reaction control (not containing enzymes) as described above [25]. The unit of NOS was expressed as 1 nmol NO formed per hour/mg protein.

The activity of the liver and kidneys arginase was evaluated by the formation of urea from arginine. Briefly, 100 μL of 200 mM arginine and 100 μL of 0.5 mM MnCl$_2$ were added to 100 μL 10% liver homogenate. The reaction was completed to 1 mL with 100 mM of sodium bicarbonate buffer, pH 9.5 and incubated at 37 ℃ for 1 h and 1 mL of 0.5 M perchloric acid was added [27]. Urea was determined to using the diacetyl monoxime method [28].

DNA fragmentation was performed according to the method described by Gerçel-Taylor [29].

Preparation of samples for histopathology
Part of the liver, kidneys and spleen were placed directly into formalin for approximately 24 h. The tissue samples were then dried, embedded in paraffin and divided at 5 mm. The wax was removed from various parts, rehydrated and treated to stain hematoxylin and eosin [30].

Statistical analysis
Excel 2013, Origin 6 and SPSS 19 were used to perform statistical analysis and plot numbers of obtained results. Values are expressed as mean±SD. One-way ANOVA with post hoc Tukey's tests were carried out. Also Ryan-Einot-Gabriel-Welsch F-test (R-E–G-WF) was performed to separate means by using SPSS program. The one way Anova F-test is to compare significant values between groups. p values less than 0.05 are considered significant.

Results and discussion
Characterization of extracted ellagic and ellagic acid nanoparticles
The ellagic acid was extracted from pomegranate and encapsulated with chitosan as the nanoparticles of ellagic acid EANP@CS. EANP@CS. The characterization has been demonstrated by FT-IR, UV, XRD diffraction, and
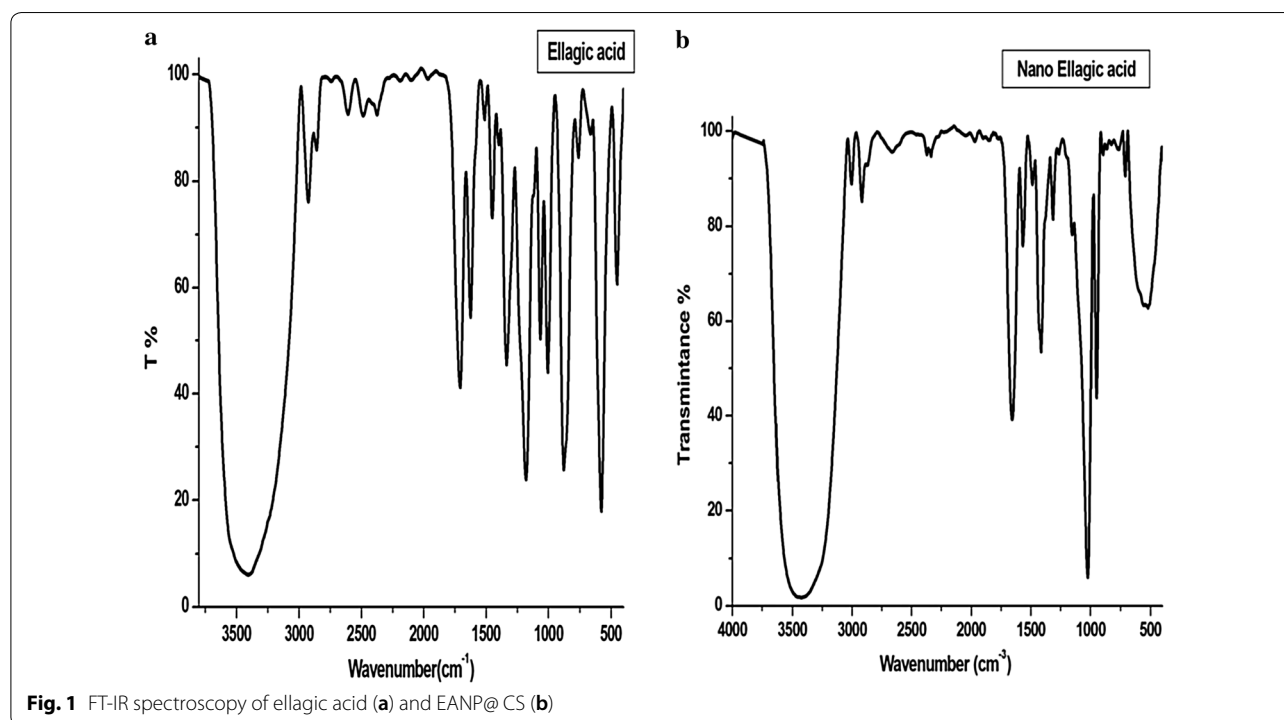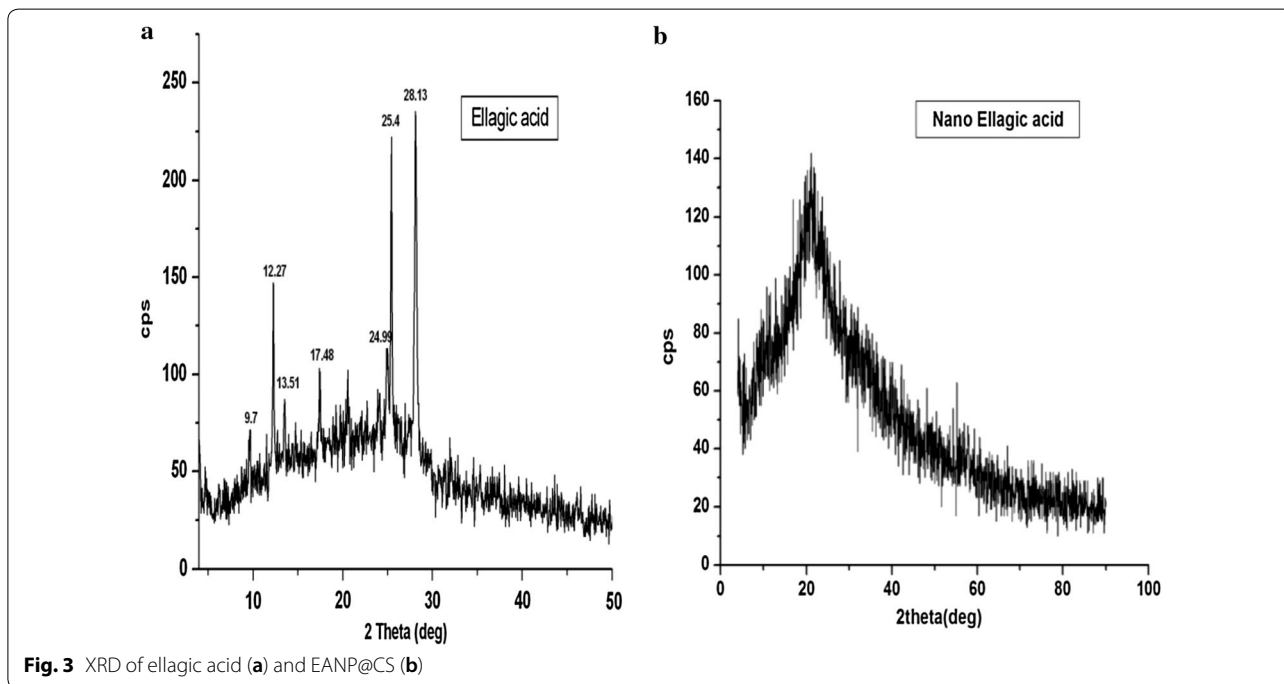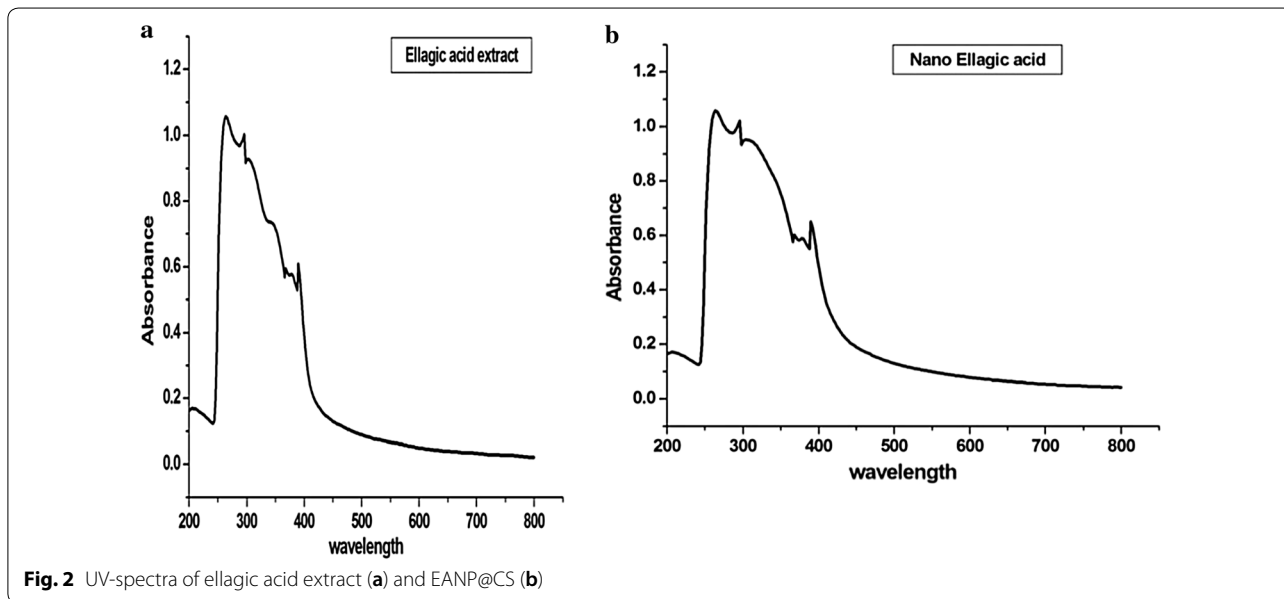

Fig. 1 FT-IR spectroscopy of ellagic acid (**a**) and EANP@ CS (**b**)

EL Barky *et al. Appl Biol Chem*   (2020) 63:47

Page 5 of 16

TEM. The FT-IR procedure was to recognize the interaction between CS and EA confirming the embodiment of EA in the nanoparticle (Fig. 1a, b). The FT-IR spectrum of ellagic acid exhibits a broadband at 3400 cm^{-1} which is attributed to the -OH expansion. While EANP@CS was shifted to 3425 cm^{-1}, the broadband C=O was changed

at 1705 cm^{-1} and in EANP@CS to 1653 cm^{-1}. The aromatic ring range observed at 1613 cm^{-1} and 1509 cm^{-1} was observed due to peak vibrations, the range at 1190 and 1052 cm^{-1} is due to the ester linkage of the expansion of C-O, and the band is assigned to 758 cm^{-1} to CH aromatic. The bending vibration and 2927 cm^{-1}

Fig. 2 UV-spectra of ellagic acid extract (**a**) and EANP@CS (**b**)

Fig. 3 XRD of ellagic acid (**a**) and EANP@CS (**b**)

EL Barky *et al. Appl Biol Chem*　(2020) 63:47

Page 6 of 16

and 2848 cm^{-1} can be attributed to the expansion of the aromatic ring CH. The shifted bands that noted in these results confirmed that the phenolic OH group had participated during the EA reaction with CS-NP. Thus, this shift at peak sites is due to the interaction between EA and CS-NP that is consistent with Arulmozhi [15].

UV spectroscopy was used to verify whether EA interference in chitosan led to changes in its optical properties. UV spectra for both ellagic and EANP@CS molecules indicated that ellagic acid has a maximum λ of 264, 295 and 393.8 (Fig. 2a, b).

XRD data for both EA and EANP@CS extracted are shown in (Fig. 3a, b) The observed diffraction peaks were at the values of theta 9.7, 12.27, 13.51, 17.48, 24.99, 25.4 and 28.13. On the other hand, EANP@CS displayed integration of peaks as a result of nano size (Fig. 3b). XRD data for the extracted EA reveal that the compound is crystalline, with a sharp and dense peak with a diffraction angle (2θ) of 28.13° and 25.4 small and dull peaks at different diffraction angles. Furthermore, the XRD of Chitosan shows two distinct crystal peaks close at 10° and 20° due to reflections 020 and 110, this may be the regularity of the polymer chain structure due to the strong hydrogen bonds between the molecules formed between the hydroxyl and amino groups present in the chitosan [31].

Electron microscopy transmittance graphs of EANP@CS coated are shown in (Fig. 4). It was observed that the size of the nanoparticles was of average size varying from 20 to 62 nm and appeared as spherical clusters in the shape. Most of the characteristic peaks of ellagic acid and chitosan appeared in the refractive patterns of EANP@CS but at low intensity. This also demonstrated that crystal penetration and Chitosan decreased but still occur as most of the drug was converted to an amorphous form during installation, EANP@CS showed the integrity of the peaks as a result of the nano-compound.
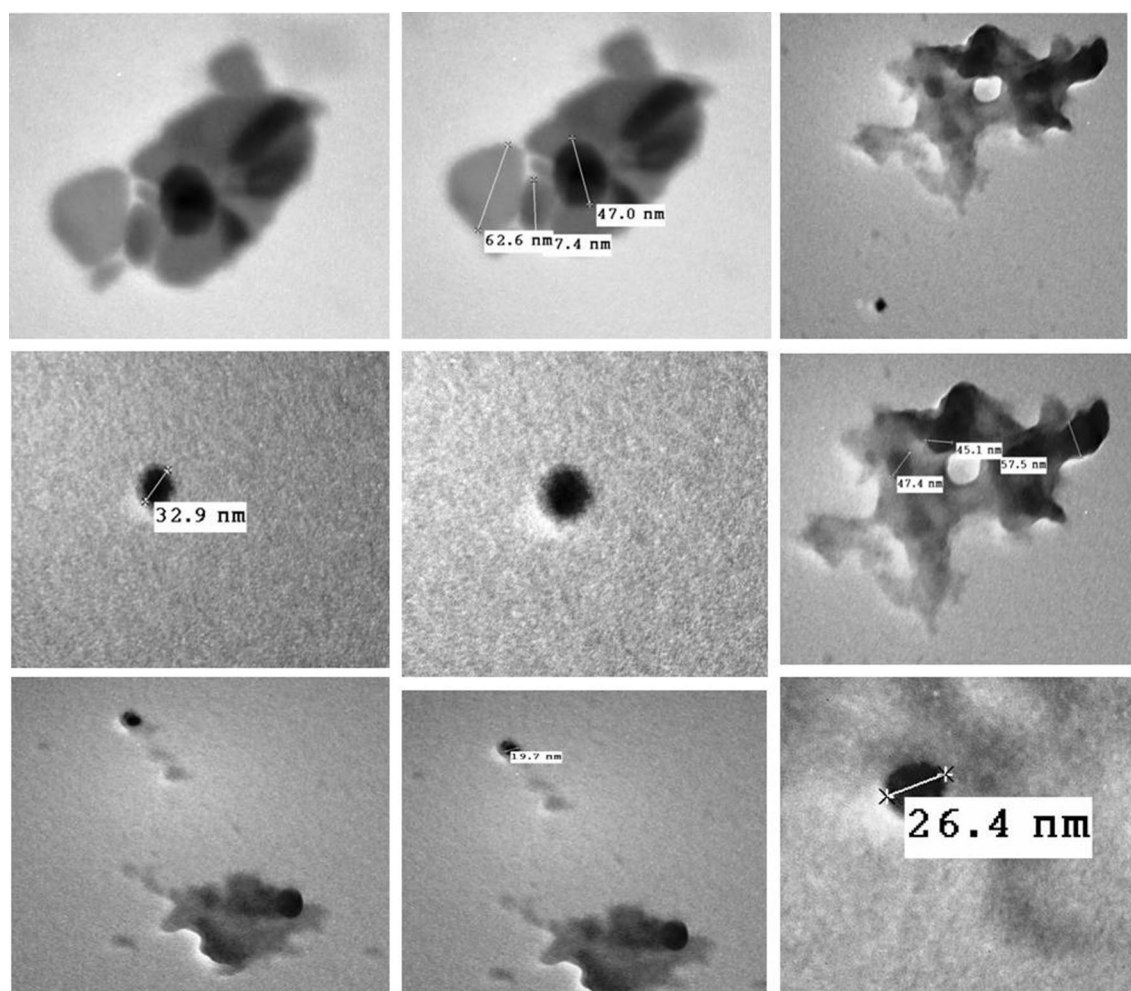

Fig. 4 Transmission electron micrographs of ellagic acid encapsulated chitosan nano particles

EL Barky *et al. Appl Biol Chem*   (2020) 63:47

Page 7 of 16

Nanoparticles covered with ellagic acid appear as groups of average molecular size ranging from 20 to 62 nm, which may be due to the tendency of chitosan molecules of ellagic acid to merge with each one through a broad hydrogen bond. The slight increase in the size of some nanoparticles can be due to the drug's incorporation between the polymeric networks [32].

Ellagic acid coated nanoparticles in target tissues were reached by passive targeting, and nanoparticles reached the target organ due to leaking connections [33].

Effect of EANP@CS on hemoglobin, liver and kidney functions, oxidant, antioxidants and nitric oxide, DNA fragmentation

Some rats under study drinking water contaminated with sodium nitrite (2 g/L) without taking EA nanoparticles for 8 weeks resulted in some of these rats died, one of them was paralyzed on one side of the body, some deformities occurred to them and two of them were tumors in their abdomen. Hemoglobin level showed a significant decrease in rats drinking the sodium nitrite

Table 1 Hemoglobin level, serum urea level and AST and ALT activities in rats drinking $NaNO_2$ and treated with EANP@CS during or stopping drinking $NaNO_2$
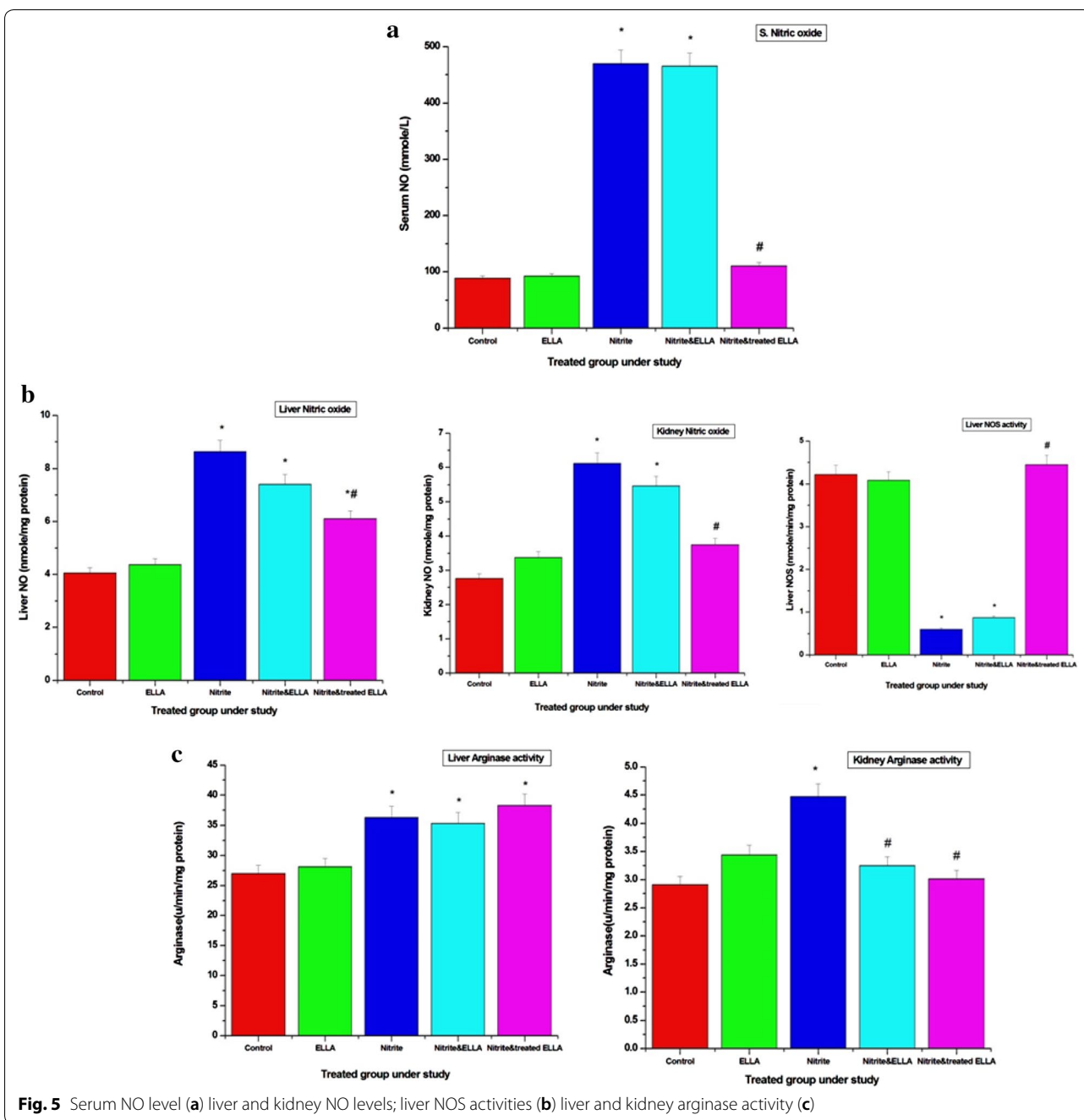
Parameters Groups	Hb (g %)	Urea (mg %)	AST (U/L)	ALT (U/L)
Group I (Control)				
Range	13.8–17.7	22.5–41.3	52–81.7	22.2–46.5
Mean ± SD	15.68 ± 1.32	32.66 ± 6.82	67.15 ± 10.25	32.39 ± 8.19
Group II (Ellagic)				
Range	13.9–16.5	25.3–41.4	55.7–82.4	25.4–45.1
Mean ± SD	15.32 ± 0.85	33.44 ± 6.05	68.3 ± 8.67	34.57 ± 5.64
p value	N.S.	N.S.	N.S.	N.S.
Group III ($NaNO_2$)				
Range	11.2–15.7	41.1–63.3	73.9–137.6	28.9–52.8
Mean ± SD	13.23 ± 1.4	50.26 ± 7.51	102.9 ± 22.98	39.52 ± 7.68
p value	< 0.001	< 0.001	< 0.001	= 0.059
Group IV ($NaNO_2$ and EANP@CS treated during drinking)				
Range	12.8–17.94	23.9–46.8	49.1–85.9	26.79–43.8
Mean ± SD	15.53 ± 1.59	38.05 ± 6.95	65.81 ± 12.62	35..67 ± 6.4
p value	N.S.	N.S.	N.S.	N.S.
*p** value	= 0.0029	= 0.00139	< 0.001	N.S.
Group V ($NaNO_2$ and treated EANP@CS after stopping) drinking)				
Range	13.8–17.36	24.51–48.8	52–85.8	28.14–44.7
Mean ± SD	15.2 ± 1.2	39.03 ± 7.01	68.53 ± 10.1	36.27 ± 5.02
p value	N.S.	N.S.	N.S.	N.S.
*p** value	= 0.0033	= 0.00282	< 0.001	N.S.

$NaNO_2$ (0.2 g %, orally); EANP@CS (20 mg/kg oral)

NS Non significant

p value versus control

*p** versus $NaNO_2$ group

group compared to the normal group. Whereas the hemoglobin level was improved to the normal level in EANP@CS-treated mice during or off drinking nitrites (Table 1). Prolonged use of sodium nitrite may result in death from methemoglobin in the blood. Moreover, low doses have had a harmful health effect, which includes birth faults, respiratory disease, nervous system injury and paralysis [34]. Prolonged ingestion of nitrite may lead to carcinogenicity and mutation [35]. Prolonged drinking of sodium nitrite may lead to toxic heme or iron, nitrite is believed to create free radicals, and oxidation of ferrous in oxyhemoglobin may form of methemoglobin. [36].

The urea level as a biomarker of kidney disease as well as serum AST activity as a biomarker for the liver, heart, and muscle showed a significant increase in mice that drink nitrite compared to normal rats. It was observed that blood urea level and AST activity showed almost normal levels and significantly decreased in rats that drink nitrite and treated it with EANP@CS during or stopping nitrite (Table 1).

Serum AST activity was high in rats that drank nitrites, possibly due to increased methemoglobin in the blood from hypoxia in liver or heart cells causing the enzymes to leak into the blood [37, 38].

Also, serum urea was higher in rats given nitrite. It indicated that the glomerular filtration rate and tubular reabsorption may decrease due to the formation of peroxynitrites [37, 38].

Nitric oxide consists of nitrates and nitrites. Food nitrate is converted to nitrite by bacteria in the large intestine and by protein enzymes containing heme and changed to nitrite. Nitrites are a reservoir of NO and bind with thiol hem- protein to form nitrosylation of hems [39].

F-test of serum NO, liver and kidney NO levels were 144.73, 16.71 and 12.93 respectively. Serum NO and liver NO levels (nitrite/nitrate) increased 5.2 folds and 2 folds respectively compared to normal rats (Fig. 5a, b). Whereas, serum NO level showed a significant decrease in EANP@CS-treated rats after nitrite was discontinued and no change was observed compared to the normal control group (Fig. 5a). On the other hand, the NO level of the liver and kidneys showed a significant decrease in EANP@CS-treated rats after nitrites were discontinued (G. V) compared to the sodium nitrite group (Fig. 5b).

It was reported that the plasma nitric oxide level increased about twice as much in rats that drink sodium nitrite by gavage (45 mg/kg/day) for 7 days [40]. Ellagic acid inhibitor the level of nitric oxide in the liver and kidneys in rats that cause alcohol and endrin substances and treated with EA [41].

On the contrary, liver activity of NOS was reduced 7 and 4.9 times in rats drinking $NaNO_2$ and rats treated

Fig. 5 Serum NO level (**a**) liver and kidney NO levels; liver NOS activities (**b**) liver and kidney arginase activity (**c**)

with EANP@CS during drinking $NaNO_2$ respectively compared to normal group. Serum or liver NO level was raised which may prevent NOS expression. F-test of liver NOS activity was 123.89. Liver NOS activity was raised in rats that drank nitrites and treated with EANP@CS after discontinuation of nitrite compared to intoxicating rats with nitrite (Fig. 5b).

Arginase prevents L-arginine from producing NO. Arginase produces ornithine forms the polyamine responsible for tissue repair and cellular growth and inhibits NOS. EA inhibits gene expression of NOS in liver cells and increase the activity of arginase in cancer cells [42].

EL Barky *et al. Appl Biol Chem*   (2020) 63:47

Page 9 of 16

F-test of liver and kidney arginase activity were 8.43 and 3.63 respectively. Liver arginase activity showed a significant increase in the sodium nitrite group, EANP@CS with and after stopping nitrites compared to the normal control. On the other hand, the renal arginase activity showed a significant increase in the sodium nitrite group compared to the normal group, but the liver arginase activity showed a significant decrease in both EANP@CS with and after stopping nitrites (G. IV and GV) compared to the sodium nitrite group (G. III) (Fig. 5c).

The spleen can produce NO when it is driven by any poison [43]. The data obtained in this study showed that the sodium nitrite group resulted in a significant increase in both the spleen NO and L-MDA compared to the normal group whereas EANP@CS significantly improved spleen disorder for each of the treated group compared to the sodium nitrite group (Data have not shown).

F-test of liver and kidney MDA level were 16.28 and 6.49 respectively. In the present study, liver and kidney MDA level was higher in rats that were drinking nitrites consistent with Adewale et al. [44]. Whereas, Liver and kidney L-MDA level showed a significant decrease in the two groups (G. IV and G. V) compared to (G. III) and showed insignificant differences between rats that treated with EANP during or discontinuation drink $NaNO_2$ Kidney L-MDA level was reduced in rats treated with EANP@CS after discontinuation of NaNO2 compared with rats that drank sodium nitrate (Fig. 6a).

Nitrite is known as a highly reactive compound that has the ability to oxidize, reduce or reduce nitrosylating compounds. It can also be converted into a trillion of the same compounds, nitrous acid, nitric oxide and nitrite [45].

Lipid peroxidation is one of the main causes of cell toxicity with sodium nitrite. Sodium nitrite binds with amines in the stomach that produce nitrosamine and free radicals. Nitrosamine can increase the lipid peroxide cell membrane, thereby dissolving the liver membrane and infecting the cell [46].

It was reported that the EA reduces the liver MDA level in skin necrosis in rats due to two groups of lactone in the EA structure that act as scavenging of free radicals and lipid peroxide [41].

Ellagic acid contains powerful antioxidants. The main antioxidant technique is direct scavenging of free radicals, nitrogen reactive species and ROS, including hydroxyl radicals, peroxyl radicals, NO_2 radicals, and peroxynitrite. Another technique involves protecting the DNA from any attack of mutation by direct combination with this large molecule, the suppression of produced ROS, and chelation of metals as copper [47].

F-test of liver and kidney GSH level (15.57 and 6.43), and liver PSH and NPSH levels (8.74 and 4.63) were observed. F-test of liver and kidney Gpx activities (20.52 and 1.491), liver and kidney GST activites (12.68 and 3.34), and liver catalase activity (16.70) were detected. The current study, liver and kidney GSH and both liver PSH and NPSH levels, and kidney and liver Gpx, GST and catalase activities showed a significant decrease in rats that drank nitrite, while these antioxidant parameters did not show changes after stopping the nitrite and treated with EANP@CS compared to control (Fig. 6b–d) and (Fig. 7). GSH may combine with nitrites or its metabolites and act as a non-enzymatic detoxification action or be catalyzed by GST. GSH was depleted as a substrate and cofactors for both GST and Gpx activities, and thus these enzymatic activities were reduced. It was reported that serum L-MDA, NO levels and GST activity were raised. On the other hand, the activities of GSH, catalase, and arginase have been depleted in rats given to nitrite [48]. Ellagic acid inhibits the oxidation of glutathione and lipid peroxidation and increases genetic expressions and Gpx, GST and catalase activities in liver cells [7].

Liver, kidney, GSH, and PSH and NSPH levels of both groups (G. IV and G. V) showed a significant increase compared to the sodium nitrite group (G. III) but did not reach the normal value (Fig. 6b–d). Liver GPx, GST and catalase activities showed a significant increase in EANP@CS-treated rats and a significant increase in kidney GST activity in (G. V) compared to rats taking sodium nitrite numbers (Fig. 7a–c).

The chemical composition of EA has conjugated double bonds and accepts electrons from free radical compounds to form stable compounds. Ellagic acids can improve antioxidant status in both liver and kidneys by scavenging superoxide, hydroxyl anion, and peroxynitrites. EA is a potent antioxidant compared to α-tocopherol and can enhance GSH-based protection. EA inhibits the cytokines produced by reactive oxygen species and inflammation [49].

F-test of hepatic DNA fragmentation was 29.54. Hepatic DNA fragmentation was raised in the sodium nitrite group (43.32%) compared to the normal group. On the other hand, the proportion of DNA fragmentation showed a significant decrease in the two groups treated with EANP@CS (G.IV and G. V) (27.30 and 26.4%), respectively (Fig. 8).The obtained data were an agreement with Sherif and Al-Gayyer [50].

Sodium nitrite causes hepatic failure through various mechanisms, for example, oxidative stress and DNA fragmentation [51]. Also, the lipid peroxide induced by the free radicals of sodium nitrite binds with DNA and thus accelerates the fragmentation of DNA [52].

The nitric oxide created as a result of daily consumption of sodium nitrite can deaminate the bases of purine and pyrimidine in the DNA, and thus can be the cause of
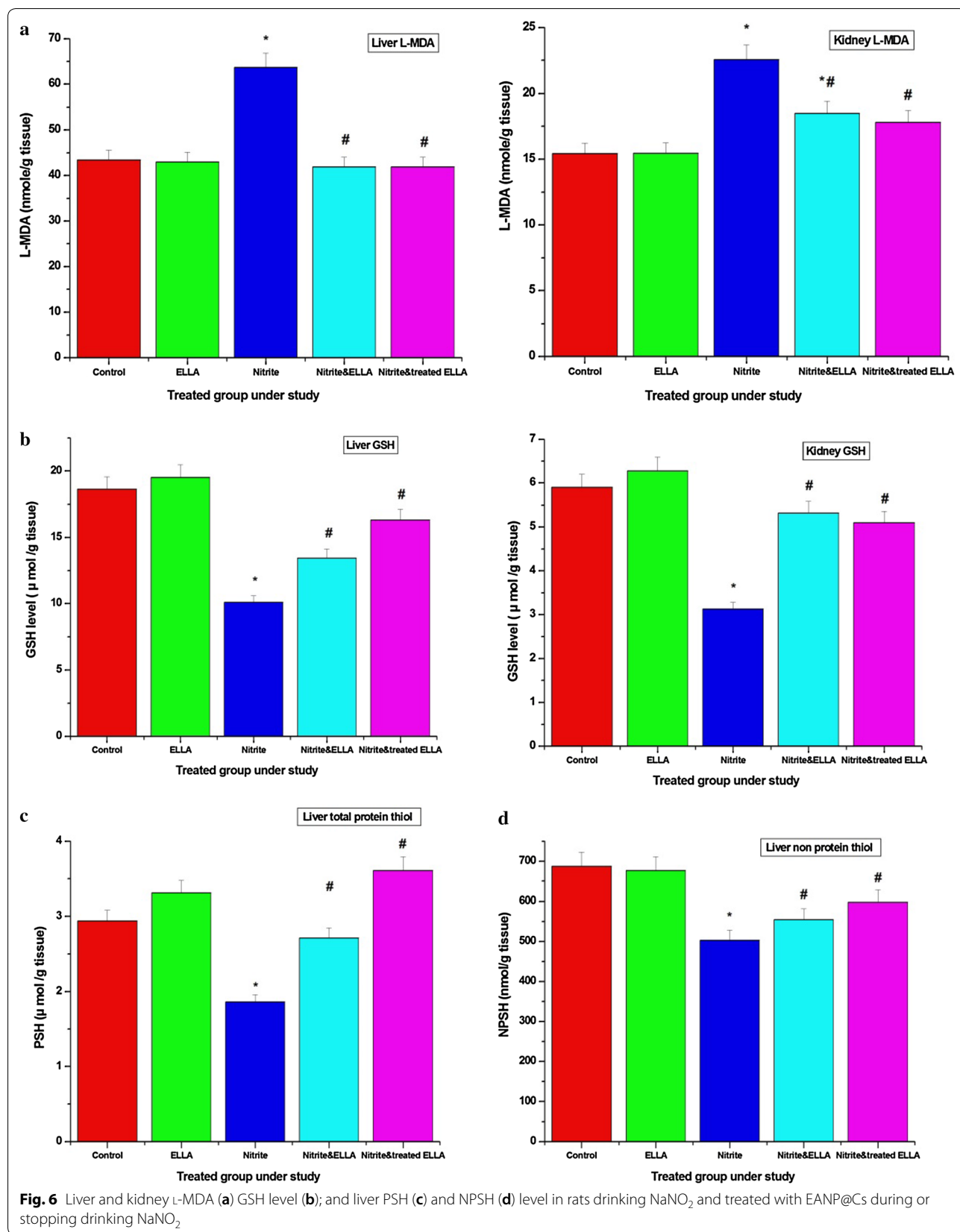
Fig. 6 Liver and kidney L-MDA (**a**) GSH level (**b**); and liver PSH (**c**) and NPSH (**d**) level in rats drinking NaNO$_2$ and treated with EANP@Cs during or stopping drinking NaNO$_2$

EL Barky *et al. Appl Biol Chem*   (2020) 63:47

Page 11 of 16

Fig. 7 Liver and kidney Gpx (**a**) GST activities (**b**), and liver catalase (**c**) in rats drinking NaNO$_2$ and treated with EANP@Cs during or stopping drinking NaNO$_2$

EL Barky *et al. Appl Biol Chem*   (2020) 63:47

Page 12 of 16

Fig. 8 Liver DNA fragmentation in rats drinking NaNO$_2$ and treated with EANP@Cs during or stopping drinking NaNO$_2$
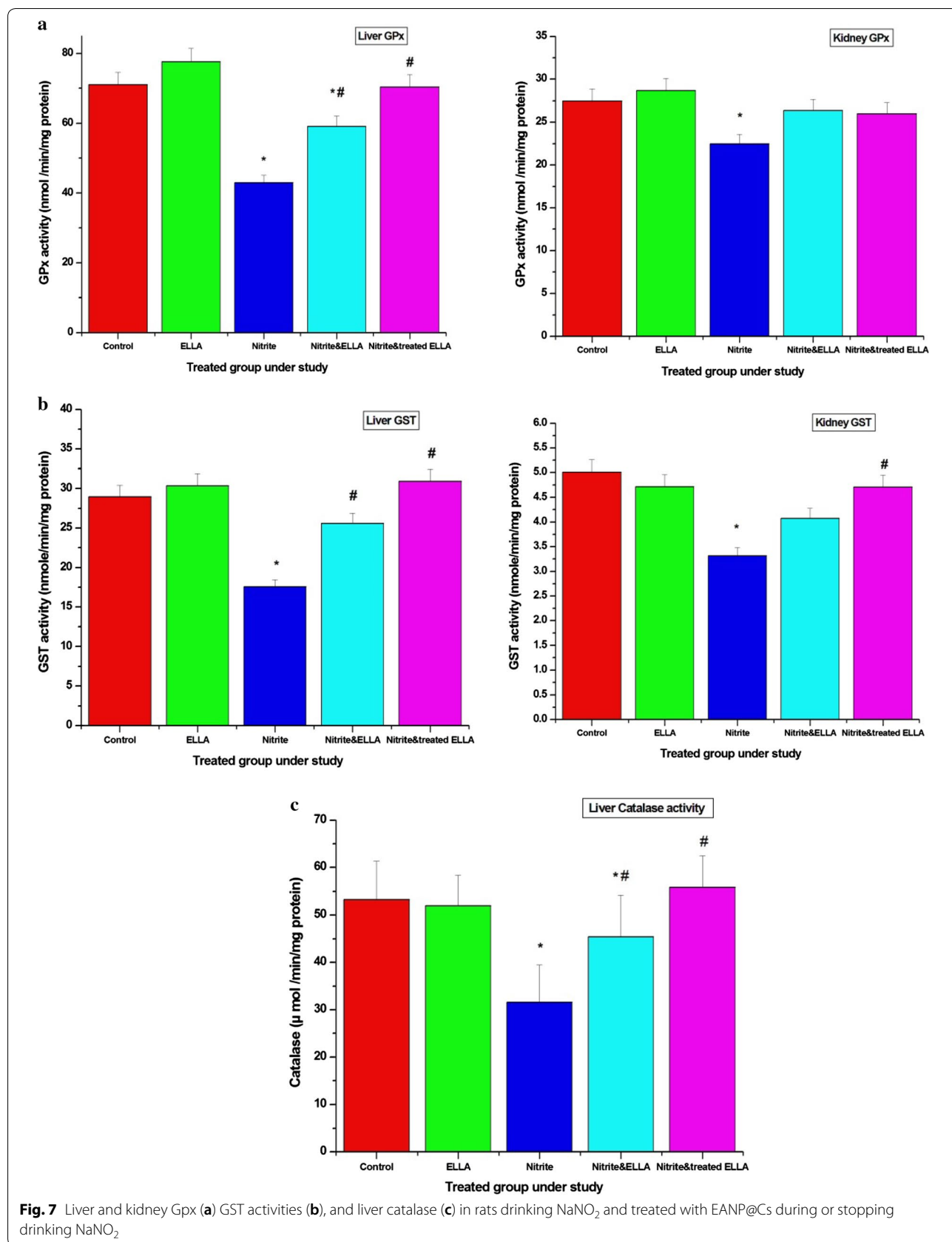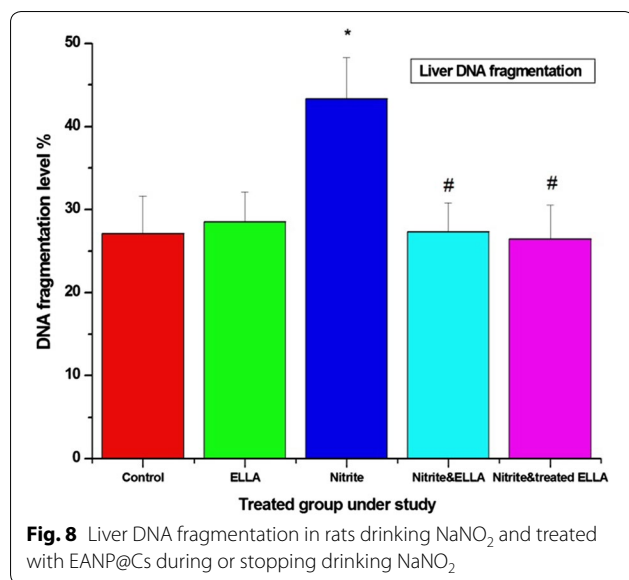
the increase in mutations and the breaking of the DNA strand [53].

Histopathology of liver, kidney, and spleen

Control of normal hepatic mice showed average pyloric ducts, and average central veins surrounded by intermediate hepatic cells arranged in single cell cords with average overlapping blood sinusoids. On the other hand, the sodium nitrite group (G. III) showed a marked expansion of the dilated central and portal veins and hepatocytes showed more marked micro- and macro-vesicular steatosis in periportal areas than peri-venular areas with an expanded portal tract by inflammatory infiltrate. Moreover, in both groups treated with EANP @ CS (G. IV and G. V) they showed central and dilated portal veins and hepatocytes showed more steatosis in the areas surrounding peri-venular than the areas surrounding the portal (Fig. 9).

Furthermore, control in normal rats of the kidney showed average renal capsule average and average glomeruli with average bowman area and average proximal tubules with preserved brush borders, average distal tubules, and average interstitial. However, in the sodium nitrite group, the kidney showed atrophied glomeruli with dilated Bowman's spaces and some proximal tubules showed loss of brush borders. The sodium nitrite group treated with EANP@CS average glomeruli with average Bowman's spaces and average proximal tubules with preserved brush borders (Fig. 10).

The spleen from the normal control group showed average lymphoid follicles (white bulb) with central arterioles, average sinusoids in the blood (red bulb), and average fibrous septa. Whether the spleen from the NaNO$_3$ group showed average lymph follicles with central arterioles and sinus dilatation in the blood with bleeding areas. The group treated with EANP@CS showed average lymphoid follicles, mildly dilated blood sinusoids and scattered giant cells (Fig. 11).

Kidney and hepatocyte infiltration and vascular degeneration were observed in rats consuming 20 mg/kg/day of nitrite for 4 weeks, and in rats that drink nitrite 200 mg/kg for 6 months. The cytoplasmic vacuolization of centrilobular hepatocytes and tubular degeneration and congestion of glomerular capillaries and swelling in glomerular cells in the kidney of mice and rats were given nitrites [37, 54]. Reactive oxygen species and nitric oxide can be the main cause of degenerative and histopathological alterations of tissues [54]. Ellagic acid can reduce
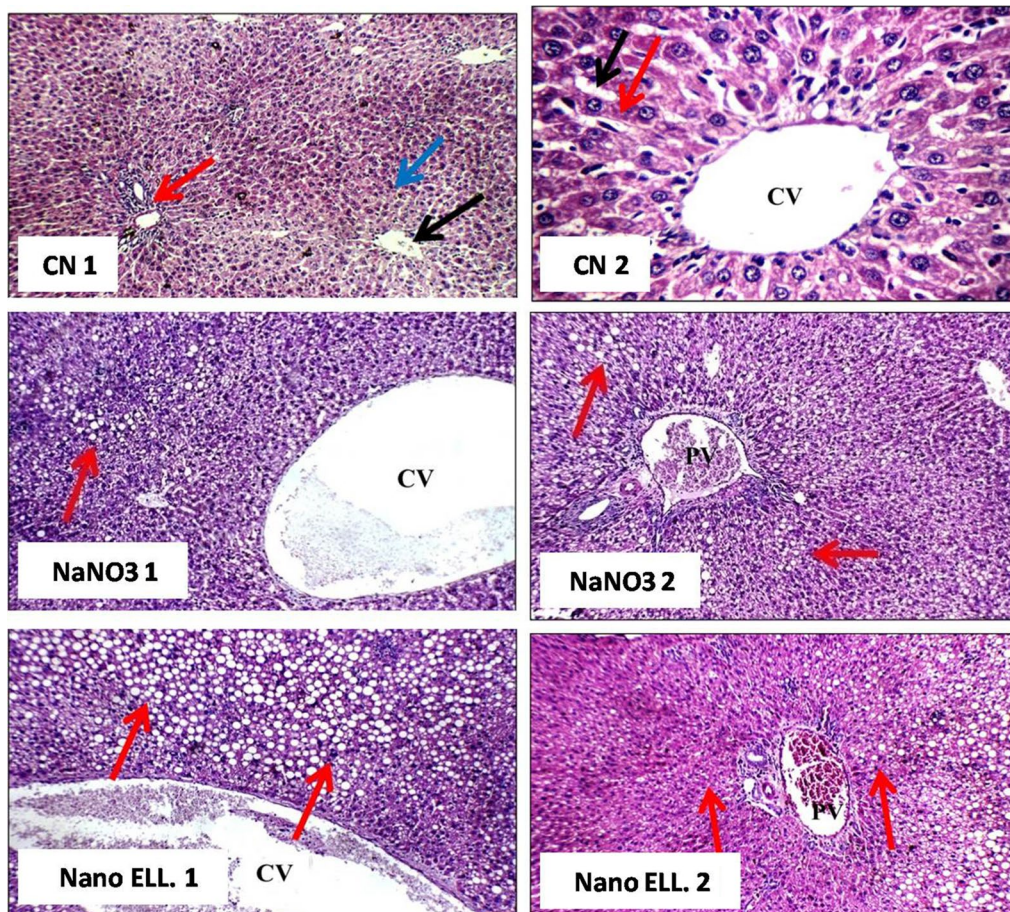
EL Barky *et al. Appl Biol Chem*   (2020) 63:47

Page 13 of 16

Fig. 9 Photomicrograph of liver stained with hematoxylin and eosin.(CN1), control group, liver showing average portal tract (red arrow), average central vein (blackarrow) surrounded by average hepatocytes (blue arrow) (H&E X 200) and (CN2) with high power view showing average central vein (CV), surrounded by average hepatocytes arranged in single-cell cords (red arrow) with average intervening blood sinusoids (black arrow) (H&E X 400). (NaNO$_3$ 1) group, liver showing markedly dilated central vein (CV) with hepatocytes showing mild steatosis (red arrow) (H&E X 200), also (NaNO$_3$ 2) showed dilated portal vein (PV) with hepatocytes showing mild to moderate steatosis (red arrows) (H&E X 200). (Nano ELL. 1) rats treated with EANP@ CS during drinking nitrites, liver showed markedly dilated central vein (CV) with hepatocytes showing marked steatosis (red arrows) (H&E X 200), also, another view of liver of rat treated with EANP@CS after stopping nitrites showed dilated portal vein (PV) with hepatocytes and mild steatosis in peri-portal area (red arrows) (H&E X 200) (Nano ELL.2)

fibrosis and inhibit the formation of NF-κB as biomarkers of inflammation in rats with diabetic nephropathy [55]. EANP@CS can be beneficial to protect against the negative effects of nitrite.

Authors' contributions
EMMA and AREB designed the protocol EMMA and AREB conducted the experiment as well as EMMA and TMM wrote the manuscript. TMM and EMMA revised the final manuscript. All authors read and approved the final manuscript.

Availability of data and materials
All data is available in the main text.

Competing interest
All the authors hereby agreed and confirm that there is no conflict of interest for this research work and publication of this paper.

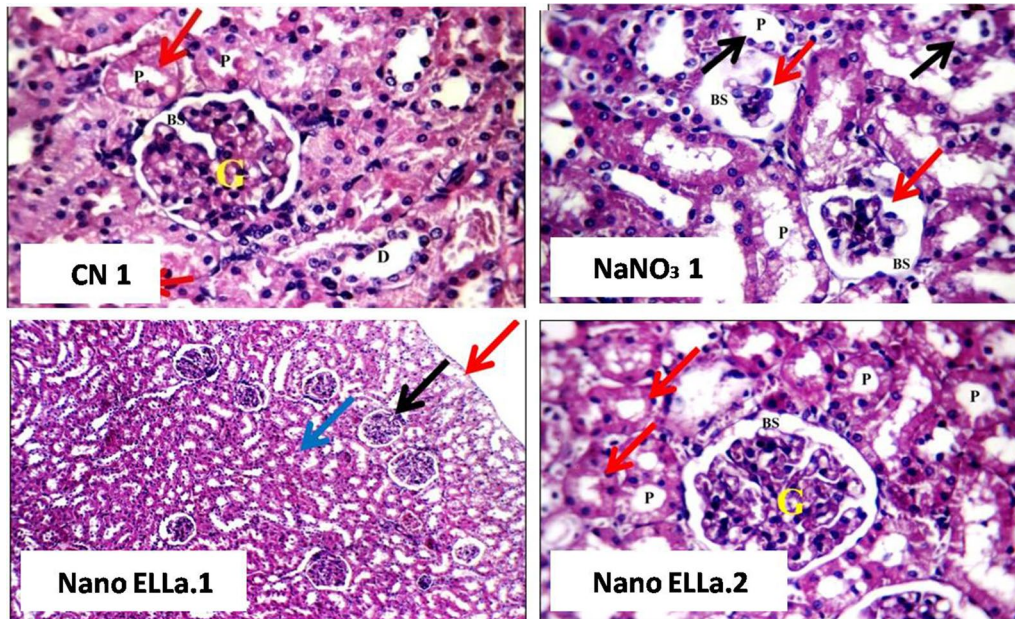EL Barky *et al. Appl Biol Chem*   (2020) 63:47

Page 14 of 16

Fig. 10 Photomicrograph of kidney stained with hematoxylin and eosin. (CN1) control group high power view showing average glomeruli (G) with average bowman's space (BS) and average proximal (P) tubules with brush borders (red arrows) and average distal tubules (D) (H&E X 400). However, (NaNO$_3$ 1) kidney high power view showing atrophied glomeruli (red arrows) with dilated Bowman's space (BS) and some proximal (P) tubules showing loss of brush borders (black arrows) (H&E X 400). (Nano ELLa.1), treated with EANP@ CS the kidney, showing average renal capsule (red arrow), average glomeruli (black arrow) and average tubules (blue arrow) (H&E X 200) and (Nano ELLa.2) high power view showing average glomerulus (G) with average bowman's space (BS) and average proximal (P) tubules with preserved brush borders (red arrows) (H&E X 400)
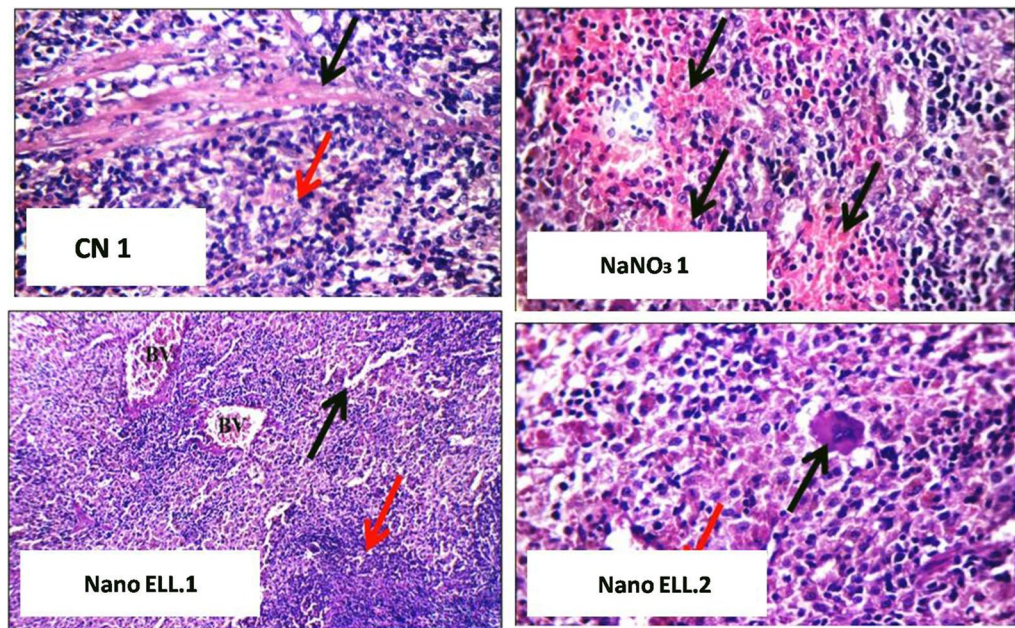

Fig. 11 Photomicrograph of spleen stained with hematoxylin and eosin. (CN1) normal group spleen high power view showing average blood sinusoids (red bulb) (red arrow), and average fibrous septa (black arrow) (H&E X 400). Meanwhile, (NaNO$_3$ 1) spleen, high power view showing areas of hemorrhage inred bulb (black arrows) (H&E X 400). (Nano ELL.1), treatment with EANP@CS acid, spleen showing average lymphoid follicles (red arrow) with mildly dilated blood sinusoids (black arrow) and dilated blood vessels(BV) (H&E X 200) and (Nano ELLa.2) of EANP@CS. High power view showing mildly dilated blood sinusoids (red arrow) with scattered giant cells (black arrow) (H&E X 400)

EL Barky *et al. Appl Biol Chem*   (2020) 63:47

Page 15 of 16

Author details
[1] Biochemistry Department, Faculty of Science, King Abdulaziz University, Jeddah, Saudi Arabia. [2] Division of Biochemistry, Chemistry Department, Faculty of Science, Tanta University, 31527 Tanta, Egypt.

References
1. Narozhnyi SV, Rozanova KD, Bobrova OM, Nardid OA (2018) Antioxidant and antiradical effects of extracts derived from cryopreserved human placenta. Probl Cryobiol Cryomed 28(4):322–332
2. Crowe W, Elliott CT, Green BD (2019) A review of the in vivo evidence investigating the role of nitrite exposure from processed meat consumption in the development of colorectal cancer. Nutrients 11(11):2673
3. De Mey E, De Maere H, Paelinck H, Fraeye I (2017) Volatile N-nitrosamines in meat products: potential precursors, influence of processing, and mitigation strategies. Crit Rev Food Sci Nutr 57(13):2909–2923
4. Ohshima H, Yoshie Y, Auriol S, Gilibert I (1998) Antioxidant and pro-oxidant actions of flavonoids: effects on DNA damage induced by nitric oxide, peroxynitrite and nitroxyl anion. Free Radical Biol Med 25(9):1057–1065
5. Pinilla M, Iglesias-Moya J, Jesús Campos M, Corpas FJ, Palma JM (2019) Pomegranate (Punica granatum L.) fruits: characterization of the main enzymatic antioxidants (peroxisomal catalase and SOD isozymes) and the NADPH-regenerating system. Agronomy 9(6):338
6. Panichayupakaranant P, Tewtrakul S, Yuenyongsawad S (2010) Antibacterial, anti-inflammatory and anti-allergic activities of standardised pomegranate rind extract. Food Chem 123(2):400–403
7. García-Niño WR, Zazueta C (2015) Ellagic acid: pharmacological activities and molecular mechanisms involved in liver protection. Pharmacol Res 97:84–103
8. Ruan J, Yang Y, Yang F, Wan K, Fan D, Wang D (2018) Novel oral administrated ellagic acid nanoparticles for enhancing oral bioavailability and anti-inflammatory efficacy. J Drug Del Sci Technol 46:215–222
9. Cerdá B, Llorach R, Cerón JJ, Espín JC, Tomás-Barberán FA (2003) Evaluation of the bioavailability and metabolism in the rat of punicalagin, an antioxidant polyphenol from pomegranate juice. Eur J Nutr 42(1):18–28
10. Divya K, Jisha M (2018) Chitosan nanoparticles preparation and applications. Environ Chem Lett 16(1):101–112
11. Perera U, Rajapakse N (2014) Chitosan nanoparticles: preparation, characterization, and applications. Springer, Seafood processing byproducts, pp 371–387
12. Behl G, Sharma M, Dahiya S, Chhikara A, Chopra M (2011) Synthesis, characterization, and evaluation of radical scavenging ability of ellagic acid-loaded nanogels. J Nanomater. https://doi.org/10.1155/2011/695138
13. Lu J, Yuan Q (2008) A new method for ellagic acid production from pomegranate husk. J Food Process Eng 31(4):443–454
14. Elzatahry A, Eldin MM (2008) Preparation and characterization of metronidazole-loaded chitosan nanoparticles for drug delivery application. Polym Adv Technol 19(12):1787–1791
15. Arulmozhi V, Pandian K, Mirunalini S (2013) Ellagic acid encapsulated chitosan nanoparticles for drug delivery system in human oral cancer cell line (KB). Colloids Surf B 110:313–320
16. Til H, Falke H, Kuper C, Willems M (1988) Evaluation of the oral toxicity of potassium nitrite in a 13-week drinking-water study in rats. Food Chem Toxicol 26(10):851–859
17. Alturkistani HA, Tashkandi FM, Mohammedsaleh ZM (2016) Histological stains: a literature review and case study. Global J Health Sci 8(3):72
18. Lowry OH, Rosebrough NJ, Farr AL, Randall RJ (1951) Protein measurement with the Folin phenol reagent. J Biol Chem 193:265–275
19. Draper HH, Hadley M (1990) [43] Malondialdehyde determination as index of lipid peroxidation methods in enzymology. Academic Press 186:421–431
20. Ellman GL (1959) Tissue sulfhydryl groups. Arch Biochem Biophys 82(1):70–77
21. Sedlak J, Lindsay RH (1968) Estimation of total, protein-bound, and non-protein sulfhydryl groups in tissue with Ellman's reagent. Anal Biochem 25:192–205
22. Gross RT, Bracci R, Rudolph N, Schroeder E, Kochen JA (1967) Hydrogen peroxide toxicity and detoxification in the erythrocytes of newborn infants. Blood 29(4):481–493
23. Habig WH, Pabst MJ, Jakoby WB (1974) Glutathione S-transferases the first enzymatic step in mercapturic acid formation. J Biol Chem 249(22):7130–7139
24. Bergmeyer H. HU Bergmeyer, ed. Methods of enzymatic analysis, Pp. 440–444. Academic Press, London and New York; 1974
25. Vodovotz Y (1996) Modified microassay for serum nitrite and nitrate. Biotechniques 20(3):390–394
26. Abdelkawy KS, Salem KA (2015) Simple method for measuring endothelial nitric oxide synthase activity in clinical researches. J Appl Pharmaceutical Sci 5(3):084–090
27. Campbell JW (1961) Studies on tissue arginase and ureogenesis in the elasmobranch, Mustelus canis. Arch Biochem Biophys 93(2):448–455
28. Marsh WH, Fingerhut B, Miller H (1965) Automated and manual direct methods for the determination of blood urea. Clin Chem 11(6):624–627
29. Gerçel-Taylor Ç, Bazzett LB, Taylor DD (2001) Presence of aberrant tumor-reactive immunoglobulins in the circulation of patients with ovarian cancer. Gynecol Oncol 81(1):71–76
30. Slaoui M, Fiette L (2011) Histopathology procedures: from tissue sampling to histopathological evaluation. Springer, Drug safety evaluation, pp 69–82
31. Mukhopadhyay P, Kundu P, Prajapati A (2016) Futuristic trends in engineering. Science, Pharmacy and Management
32. Gopalakrishnan D, Damien D, Shaijumon MM (2014) MoS2 quantum dot-interspersed exfoliated MoS2 nanosheets. ACS Nano 8(5):5297–5303
33. Varshosaz J, Farzan M (2015) Nanoparticles for targeted delivery of therapeutics and small interfering RNAs in hepatocellular carcinoma. World J Gastroenterol 21(42):12022
34. Bryan NS, Loscalzo J. Nitrite and nitrate in human health and disease: Springer; 2011
35. Zhou L, Zahid M, Anwar MM, Pennington KL, Cohen SM, Wisecarver JL et al (2016) Suggestive evidence for the induction of colonic aberrant crypts in mice fed sodium nitrite. Nutr Cancer 68(1):105–112
36. Baky NAA, Zaidi ZF, Fatani AJ, Sayed-Ahmed MM, Yaqub H (2010) Nitric oxide pros and cons: the role of L-arginine, a nitric oxide precursor, and idebenone, a coenzyme-Q analogue in ameliorating cerebral hypoxia in rat. Brain Res Bull 83(1–2):49–56
37. Fouad SS, MohiEldin MM, Haridy MA, Khalil AM (2017) Ameliorative effects of ascorbic acid (vit C.) against sodium nitrite toxicity in albino rats: hematological, biochemical and histopathological studies. Am-Eurasian J Toxicol Sci 9(1):01–06
38. Talas ZS, Gogebakan A, Orun I (2013) Effects of propolis on blood biochemical and hematological parameters in nitric oxide synthase inhibited rats by Nω-Nitro-L-arginine methyl ester. Pak J Pharm Sci 26(5):915–919
39. Tepper J, Ochoa R, Rix P, Elliott G, Hoglen N, Poulin D et al (2014) A 26-week toxicity assessment of AIR001 (sodium nitrite) by inhalation exposure in rats and by intravenous administration in dogs. Int J Toxicol 33(3):162–174
40. Gonçalves-Rizzi VH, Nascimento RA, Possomato-Vieira JS, Dias-Junior CA (2016) Sodium nitrite prevents both reductions in circulating nitric oxide and hypertension in 7-day lead-treated rats. Basic Clin Pharmacol Toxicol 118(3):225–230
41. Devipriya N, Srinivasan M, Sudheer A, Menon V (2007) Effect of ellagic acid, a natural polyphenol, on alcohol-induced prooxidant and antioxidant imbalance: a drug dose dependent study. Singapore Med J 48(4):311
42. Rath M, Müller I, Kropf P, Closs EI, Munder M (2014) Metabolism via arginase or nitric oxide synthase: two competing arginine pathways in macrophages. Front Immunol 5:532
43. Sosroseno W (2000) Nitric oxide production by murine spleen cells stimulated with porphyromonas gingiva/is-derived lipopolysaccharide. Asian Pac J Allergy Immunol 18(4):209
44. Adewale OO, Samuel ES, Manubolu M, Pathakoti K (2019) Curcumin protects sodium nitrite-induced hepatotoxicity in Wistar rats. Toxicol Rep 6:1006–1011

EL Barky *et al. Appl Biol Chem*   (2020) 63:47

Page 16 of 16

45. Honikel K-O (2008) The use and control of nitrate and nitrite for the processing of meat products. Meat Sci 78(1–2):68–76

46. Akhzari M, Shafiee SM, Rashno S, Akmali M. Berberine Attenuated Oxidative Stress Induced by Sodium Nitrite in Rat Liver. Jundishapur Journal of Natural Pharmaceutical Products. 2019;14(1)

47. Gerhäuser C, Klimo K, Heiss E, Neumann I, Gamal-Eldeen A, Knauft J et al (2003) Mechanism-based in vitro screening of potential cancer chemopreventive agents. Mutation Res Fund Mol Mechan Mutagen 523:163–172

48. El-Sheikh NM, Khalil FA (2011) L-Arginine and ʟ-glutamine as immunonutrients and modulating agents for oxidative stress and toxicity induced by sodium nitrite in rats. Food Chem Toxicol 49(4):758–762

49. Williams DJ, Edwards D, Pun S, Chaliha M, Sultanbawa Y (2014) Profiling ellagic acid content: the importance of form and ascorbic acid levels. Food Res Int 66:100–106

50. Sherif IO, Al-Gayyar MM (2013) Antioxidant, anti-inflammatory and hepatoprotective effects of silymarin on hepatic dysfunction induced by sodium nitrite. Eur Cytokine Netw 24(3):114–121

51. Salama MF, Abbas A, Darweish MM, El-Hawwary AA, Al-Gayyar MM (2013) Hepatoprotective effects of cod liver oil against sodium nitrite toxicity in rats. Pharmaceutical Biol 51(11):1435–1443

52. Khan RA, Khan MR, Sahreen S (2012) CCl 4-induced hepatotoxicity: protective effect of rutin on p53, CYP2E1 and the antioxidative status in rat. BMC Complement Altern Med 12(1):178

53. Nguyen T, Brunson D, Crespi C, Penman B, Wishnok J, Tannenbaum S (1992) DNA damage and mutation in human cells exposed to nitric oxide in vitro. Proc Natl Acad Sci 89(7):3030–3034

54. Özen H, Kamber U, Karaman M, Gül S, Atakişi E, Özcan K et al (2014) Histopathologic, biochemical and genotoxic investigations on chronic sodium nitrite toxicity in mice. Exp Toxicol Pathol 66(8):367–375

55. Ahad A, Ganai AA, Mujeeb M, Siddiqui WA (2014) Ellagic acid, an NF-κB inhibitor, ameliorates renal function in experimental diabetic nephropathy. Chem Biol Interact 219:64–75

Publisher's Note